

# Interference of overlap-free entangled photons with a Mach-Zehnder-like interferometer

Xian-Min Jin<sup>1,3</sup>, Cheng-Zhi Peng<sup>1,2</sup>, Tao Yang<sup>1</sup> and Youjin Deng<sup>1,3</sup>

<sup>1</sup> Hefei National Laboratory for Physical Sciences at Microscale and Department of Modern Physics, University of Science and Technology of China, Hefei, Anhui, 230027, PR China

<sup>2</sup> Physics Department, Tsinghua University, Beijing 100084, PR China

E-mail: <sup>3</sup>jinxm@ustc.edu.cn; yjdeng@ustc.edu.cn

PACS numbers: 03.67.Bg, 42.50.Dv, 42.50.St

**Abstract.** Using spontaneous parametric down conversion and a 50:50 beam splitter, we generate coaxial polarization-entangled photon pairs, of which the two photons are far separated from each other. The photons are then sent one by one through one port of a modified Mach-Zehnder interferometer. We observe interference fringes with a periodicity half of the single-photon wavelength, independent of the distance between the photons. This feature can find applications in quantum-enhanced measurement.

## 1. Introduction

NOON state is a path-entangled state of  $N$  photons of form  $|N0 :: 0N\rangle = 1/\sqrt{2} (|N\rangle_a|0\rangle_b + |0\rangle_a|N\rangle_b)$ , where  $a$  and  $b$  are two spatial modes. In the past decades, NOON state has attracted much research interest, and a variety of interferometric applications has been found[1], including quantum lithography[2, 3] and Heisenberg-limited phase measurement[4, 5, 6]. The advantage of NOON state for metrology can be understood in the concept of photonic de Broglie wavelength[7]. Within this concept, the  $N$  photons in state  $|N0 :: 0N\rangle$  are treated as a Bose-condensate ensemble, and thus have an effective de Broglie wavelength  $\lambda/N$ , with  $\lambda$  the single-photon wavelength. This is analogous to the case of a heavy massive molecule of  $N$  atoms. As an application, NOON state can be used for phase measurement which has a precision of order  $1/N$ —the Heisenberg limit, beating the standard quantum limit  $1/\sqrt{N}$  that arises from statistical fluctuations[8].

A number of experimental observations of the photonic de Broglie wavelength  $\lambda/N$  have been reported, employing double-slit geometry[9], Mach-Zehnder (MZ) interferometer[10, 11, 12, 13], or other multi-particle interferometer[14, 15]. In experiments using MZ interferometer, which is involved in most quantum-enhanced phase measurements, Hong-Ou-Mandel (HOM) interference[16] is usually applied to suppress unwanted contributions. For  $N = 2$ , when the wave packets from the two input ports of the MZ interferometer arrive simultaneously, the pure NOON state  $|20 :: 02\rangle$  is generated. For  $N > 2$ , generating a pure NOON state by HOM interference becomes more difficult; in many cases, even if the wave packets overlap completely, the produced state is not a pure NOON state. For instance, the state prepared for phase measurement in Ref.[13] is  $\sqrt{3/4} |40 :: 04\rangle + \sqrt{1/4} |22\rangle$ , of which the last term is undesired and may decrease the associated measurement precision.

In this work, we aim to circumvent the requirement that the wave packets should at least partly overlap at the front of the MZ interferometer to generate a NOON state. This is possible because: 1), in addition to path entanglement, one can also use other degrees of entanglement, and 2), the de Broglie wavelength  $\lambda/N$  of NOON state does not depend on the spatial distribution of the involved  $N$  particles, as demonstrated in Ref.[14].

## 2. Experimental Set-up

The setup of our experiment is schematically shown in Fig. 1. It contains two parts: the photon-source generator (Fig. 1a) which produces polarization-entangled photon pairs and aligns the photons into a co-axis, and a modified MZ interferometer (Fig. 1b).

In Fig. 1a, a semiconductor blue laser beam (power  $34.5mw$ , waist  $100\mu m$ , and central wavelength  $405nm$ ) is incident on a  $2mm$ -barium-borate (BBO) crystal. As a consequence, pairs of polarization-entangled photons are generated via type-II SPDC[17], of which the central wavelength is  $810nm$ . The down-converted extraordinary and ordinary photons have different propagating velocities, and travel along different paths inside the crystal due to birefringent effect of the BBO crystal. The resulting walk-off effects are then compensated by a combination of a half wave plate (HWP) and an additional  $1mm$  BBO crystal in each arm. Photons are collected by single mode fibers (SMF). The count rate is about  $80k/s$  in each arm, and the coincidence is about  $20k$  pairs per second. As a result, we prepare the polarization

Interference of overlap-free entangled photons with a Mach-Zehnder-like interferometer<sup>3</sup>

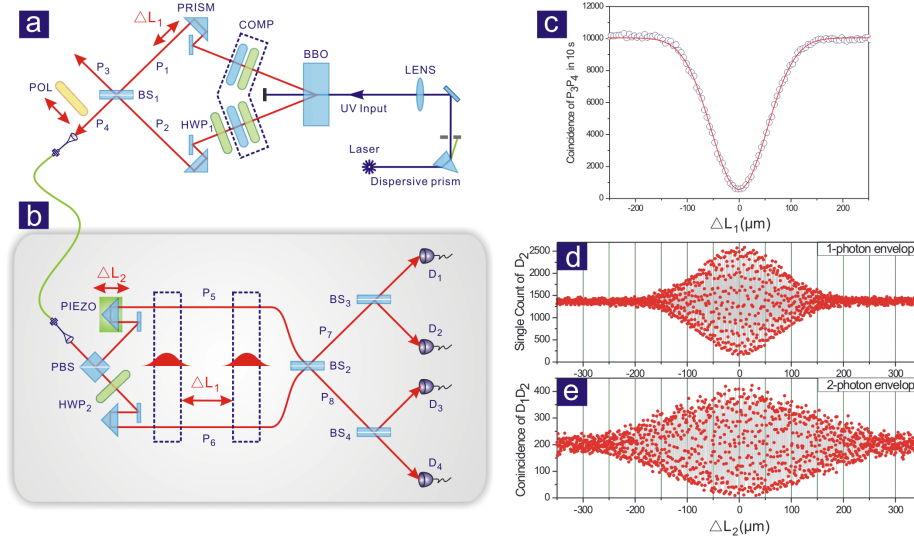


**Figure 1.** Schematic experimental setup and interference searching. (a). Preparation of coaxial polarization-entangled state  $|\Phi^+\rangle_{P_4}$  by Eq. (2). Polarization entanglement comes from the process of spontaneous parametric down conversion by pumping a nonlinear crystal. BS1 serves as a optical mixer coupling entangled photons to path P4.  $\Delta L_1$  is tuned by adjusting micrometer-resolution prism. (b). A modified Mach-Zehnder interferometer. (c). The curve for HOM interference at BS1, which displays two-photon coincidence rate versus the relative optical delay between the interfering photons  $\Delta L_1$ . (d), (e). one- and two-photon interference envelope. BBO:  $\beta$ -barium-borate crystal; HWP: half wave plate; COMP: HWP and BBO(1mm); POL: polarization plate; BS: beam splitter; PBS: polarization beam splitter; PIEZO: piezo ceramics

entanglement as

$$|\Phi^+\rangle_s = 1/\sqrt{2} (|H\rangle_1|H\rangle_2 + |V\rangle_1|V\rangle_2) , \quad (1)$$

where where  $|H\rangle(|V\rangle)$  denotes horizontal (vertical) polarization, the subscripts 1 and 2 specify spatial modes, and subscript  $s$  means state of source. The visibilities for the polarization correlations are about 98.1% for  $|H\rangle/|V\rangle$  basis and 92.6% for  $|+45^\circ\rangle/|-45^\circ\rangle$  basis, without the help of narrow bandwidth interference filters. This implies that we have produced a high-quality polarization-entangled photonic source. The photons from pathes P1 and P2 are combined at a 50:50 beam splitter (BS). A prism-built-in manual translation stage is placed on path P1 to adjust the path difference  $\Delta L_1$ , of which the precision is of order  $\mu\text{m}$ . The photons along path P4 are then guided into one port of the modified MZ interferometer (Fig. 1b).

The photon state on path P4 is usually a mixed state, depending on the path difference  $\Delta L_1$ . When  $\Delta L_1 \geq \xi$  with  $\xi$  the single-photon coherent length, the wave packets do not overlap at BS1 and each photon has the same probability to transmit or be reflected. Thus, the photon state on P4 can be a single-photon state  $H$  and  $V$  with probability 1/4, respectively, or the maximally polarization-entangled state with probability 1/4. The entanglement is also at the temporal mode, let  $t_1 \leq t_2$  specify

the time that the two photons arrive at the polarization beam splitter (PBS) of the modified MZ interferometer (Fig. 1b), and the state can be written as

$$|\Phi^+\rangle_{P4} = 1/\sqrt{2} (|H\rangle_{t1}|H\rangle_{t2} + |V\rangle_{t1}|V\rangle_{t2}) , \quad (2)$$

where subscript  $P4$  refers to path  $P4$ . When interval  $\Delta L_1 < \xi$ , the HOM interference occurs. In particular, when  $\Delta L_1 = 0$  i.e., the two wave packets completely overlap at BS1, the state that a photon is on path  $P3$  and the other on  $P4$  is eliminated, and the state on  $P4$  is a pure state described by Eq. (2).

The HOM interference curve is obtained by scanning the position of prism and measuring the coincidence at two output modes  $P3$  and  $P4$ , as shown in Fig. 1c. The visibility is determined as  $V_{HOM} = (C_{plat} - C_{dip})/C_{plat} = (94.5 \pm 0.4)\%$ , where  $C_{plat}$  is the noncorrelated coincidence rate at the plateau and  $C_{dip}$  is the interfering coincidence rate at the dip. Such a high visibility suggests that we have established accurate spatial and temporal overlap for the two entangled photons. Further, the interference curve in Fig. 1c can be approximately described by a Gaussian function, which yields the single-photon coherent length  $\xi \approx 126\mu m$ .

The setup in Fig. 1b is obtained by replacing the front BS of the standard MZ interferometer by a PBS and a HWP set at  $45^\circ$ . A manual translation stage with micrometer precision and a piezo ceramics of precision  $1nm$  is placed on path  $P5$  to adjust the path difference  $\Delta L_2$ . The two pathes are combined again at BS2. Additional two BSs are placed on pathes  $P7$  and  $P8$ , respectively, and avalanche photo diodes are used for photon detection.

Figure 1b can be regarded as a modified MZ interferometer. Consider a single-photon state  $|+45^\circ\rangle = 1/\sqrt{2} (|H\rangle + |V\rangle)$ . The horizontally polarized part  $H$  will transmit through the PBS onto path 6, and while the vertically polarized part will be reflected onto path 5. Thus, after the PBS, the state is  $1/\sqrt{2} (|V\rangle_5 + |H\rangle_6)$ . Then, the HWP will erase polarization information by rotating  $H$  to  $V$  at path 6. Taking into account the phase difference due to interval  $\Delta L_2$ , the photon state becomes  $1/\sqrt{2} (|1\rangle_5|0\rangle_6 + e^{i\phi}|0\rangle_5|1\rangle_6)$ . Similar analysis yields that a  $N$ -photon Greenberger-Horne-Zeilinger (GHZ) state[18]  $1/\sqrt{2}(|H\rangle_1|H\rangle_2 \cdots |H\rangle_N + |V\rangle_1|V\rangle_2 \cdots |V\rangle_N)$  on path 4 will be transferred into a state immediately before BS2 as  $1/\sqrt{2} (|N\rangle_5|0\rangle_6 + e^{iN\phi}|0\rangle_5|N\rangle_6)$ . Clearly, such an action for  $N = 1$  and  $N = 2$  is analogous to previous experiments in a standard MZ interferometer.

### 3. Experimental results

We carried out a few experiments, for a single-photon self-interference and the interference of the polarization-entangled pairs with various  $\Delta L_1$ , respectively. Some of these experiments are mainly for testing purposes and the others are to demonstrate the interference of overlap-free entangled photons

#### 3.1. Single-photon interference

In this experiment, the BS1 in Fig. 1a is replaced by a polarization plate (POL) oriented at  $+45^\circ$ , and thus the photon state on path  $P4$  becomes the linear polarization state  $|+45^\circ\rangle = 1/\sqrt{2}(|H\rangle + |V\rangle)$ . As described earlier, the state before BS2 is  $1/\sqrt{2} (|1\rangle_5|0\rangle_6 + e^{i\phi}|0\rangle_5|1\rangle_6)$ . After interfering at BS2, ideally, the probability to detect the single photon on path  $P7$  is  $P_7 = (1 + \cos \phi)/2$ , with  $\phi = \Delta L_2/\lambda$ , and the probability on path  $P8$  is  $P_8 = (1 - \cos \phi)/2$ .

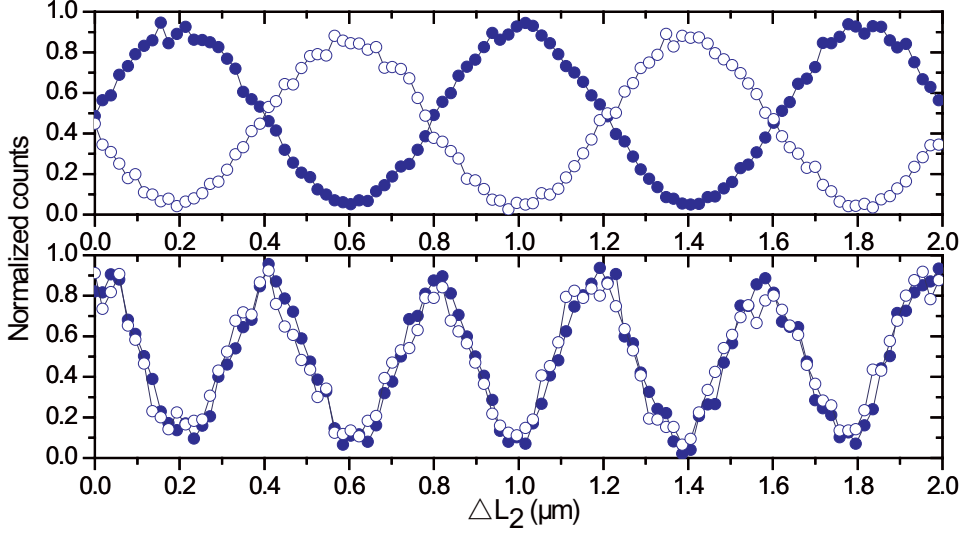


**Figure 2.** Characteristics of one- and two-photon interference. (a). one-photon count rate at path P7 (blue solid circles) and at P8 (blue open circles) as the interval  $\Delta L_2$  is varied. (b). Two-photon coincidental detection rates of  $D_1D_2$  (blue solid circles) and  $D_3D_4$  (blue open circles) versus  $\Delta L_2$ .

We first scanned  $\Delta L_2$  in a large range and obtain an interference envelope shown in Fig. 1d. This envelope was actually used to calibrate the parameter  $\Delta L_2$ :  $\Delta L_2 = 0$  corresponds to the position at the middle of the interference envelope where the interference amplitude is maximal. Further, the single-photon coherent length  $\xi$  can be obtained as the Full width at half maximum (FWHM) of the envelope, which is about  $130\mu\text{m}$ , consistent with the result deduced from the HOM interference (Fig 1.c).

We then set  $\Delta L_2 \approx 0$  and scanned the piezo ceramics with a step of 10nm. Indeed, the counting rates on Path P7 and P8 were observed to oscillate with periodicity  $\lambda = 810\text{nm}$ , as shown in Fig. 2a. The curves are of high quality and well described by  $[1 \pm \cos(\Delta L_2/\lambda)]/2$ .

### 3.2. Interference of entangled photon pairs with $\Delta L_1 = 0$

With interval  $\Delta L_1 = 0$ , the wave packets of the entangled photons arrive simultaneously at BS1 and the PBS, and the state immediately before BS2 is  $1/\sqrt{2}(|2\rangle_5|0\rangle_6 + e^{i2\phi}|0\rangle_5|2\rangle_6)$ . After BS2, the state becomes  $1/\sqrt{8}((1 - e^{i2\phi})|2\rangle_7|0\rangle_8 - (1 - e^{i2\phi})|0\rangle_7|2\rangle_8 - \sqrt{2}i(1 + e^{i2\phi})|1\rangle_7|1\rangle_8)$ . Therefore, the probability for both photons on path P7 or P8 is  $P_7 = P_8 = (1 - \cos(2\phi))/4$ , and the probability for one photon on P7 and the other on P8 is  $(1 + \cos(2\phi))/2$ . These probabilities are measured by the coincidence rate of  $D_1D_2$ ,  $D_3D_4$ , and  $D_2D_3$ , respectively.

We first varied  $\Delta L_2$  within a big range to determine the interference envelope, shown in Fig. 1e. Clearly, this envelope is much wider than that for the single-photon self-interference in Fig. 1d. The FWHM of the interference envelope in Fig. 1e is about  $300\mu\text{m}$ . To our knowledge, this is first determination of the full interference envelope of a photonic de Broglie wave.

The interference fringes of the entangled photon pairs is obtained by varying  $\Delta L_2$

near the middle of the envelope with a step of  $10nm$ . The coincidence rates of  $D_1D_2$  and  $D_3D_4$  are shown in Fig. 2b. Indeed, the oscillation periodicity is  $\lambda/2 \approx 400nm$ . The two oscillation curves also have the same phase, as predicted earlier. This confirms the concept of photonic de Broglie wave for NOON state.

### 3.3. Interference of entangled photon pairs with $\Delta L_1 \neq 0$

To demonstrate how the two-photon interference looks like for  $\Delta L_1 \neq 0$ , we theoretically consider the limiting case  $\Delta L_1 \gg 0$  such that one photon in the entangled pair described by Eq. (2) has already been detected while the other one is still before the PBS in Fig. 1b. Simple analysis yields that the state is

- immediately before BS2:  $1/\sqrt{2} (|H\rangle_{t2}|1\rangle_{6,t1} + e^{i\phi}|V\rangle_{t2},|1\rangle_{5,t1})$ ,
- immediately after BS2:  $1/2 [(|H\rangle_{t2} - e^{i\phi}|V\rangle_{t2}) |1\rangle_{7,t1} + (|H\rangle_{t2} + e^{i\phi}|V\rangle_{t2}) |1\rangle_{8,t1}]$ .

Therefore, with equal probability  $1/2$ , the first photon will be detected on path P7 or P8. Accordingly, the wave packet collapses onto  $1/\sqrt{2}(|H\rangle_{t2} \pm e^{i\phi}|V\rangle_{t2})$ , where  $\pm$  represents the two cases, respectively. Some calculations give that the state of the second photon immediately after BS2 is

$$1/2 [(1 \mp e^{i2\phi}) |1\rangle_{7,t2} + (1 \pm e^{i2\phi}) |1\rangle_{8,t2}] . \quad (3)$$

This means that the probability for both the first and the second photon travelling along the same path (either P7 or P8) is  $P_7 = P_8 = (1 + \cos 2\phi)/2$ , and that the two photons travel along the different paths with probability  $(1 - \cos 2\phi)/2$ . This is the same as the case  $\Delta L_1 = 0$ .

In short, it is plausible to expect that the coincidence rate  $\propto 1 + \cos 2\phi$  of  $D_1D_2$  and  $D_3D_4$  does not depend on the interval  $\Delta L_1$ . In the present experiment setup, the only effect of  $\Delta L_1$  is to affect the efficiency of preparing the state by Eq. (2). In addition to  $\Delta L_1 = 0$ , we carried out experiments for  $\Delta L_1 = 200\mu m$  and  $10000\mu m$ . The interval  $\Delta L_1 = 200\mu m$  is larger than the single-photon coherent length  $\xi \approx 126\mu m$  but still within the coherent length of the pump laser  $\xi_{\text{pump}} \approx 300\mu m$ , while  $\Delta L_1 = 1000\mu m$  is significantly larger than  $\xi_{\text{pump}}$ .

Figure 3 shows the coincidence rates for  $D_1D_2$  as a function of  $\Delta L_2$ . In all the three cases, the periodicity is always about  $400nm$ , half of the single-photon wavelength  $\lambda = 810nm$ . This confirms our expectation mentioned above. Nevertheless, the amplitude of the coincident events decreases as  $\Delta L_1$  becomes larger. For  $\Delta L_1 < \xi$ , HOM interference occurs, which improves the efficiency of the preparation of state by Eq. (2). For  $\Delta L_1 > \xi$ , the coupling efficiency to SMF becomes dominant. In particular, the displacement  $\Delta L_1 = 10000\mu m$  significantly exceeds the Rayleigh length defined by our SMF, and thus leads to the suppression of the coincidence rate without readjustment. To quantify the quality of the interference, we define

$$V = (C_{max} - C_{min}) / (C_{max} + C_{min}) , \quad (4)$$

where  $C_{max}(C_{min})$  is the correlated coincidence rate at the peak (valley) of the two-fold coincidence curve. In our experiment,  $V$  values calculated from sinusoidal interference fringes are  $0.98 \pm 0.01$ ,  $0.95 \pm 0.03$ ,  $0.98 \pm 0.03$  respectively. This suggests that the interference fringes in Fig. 3 are all of high quality.

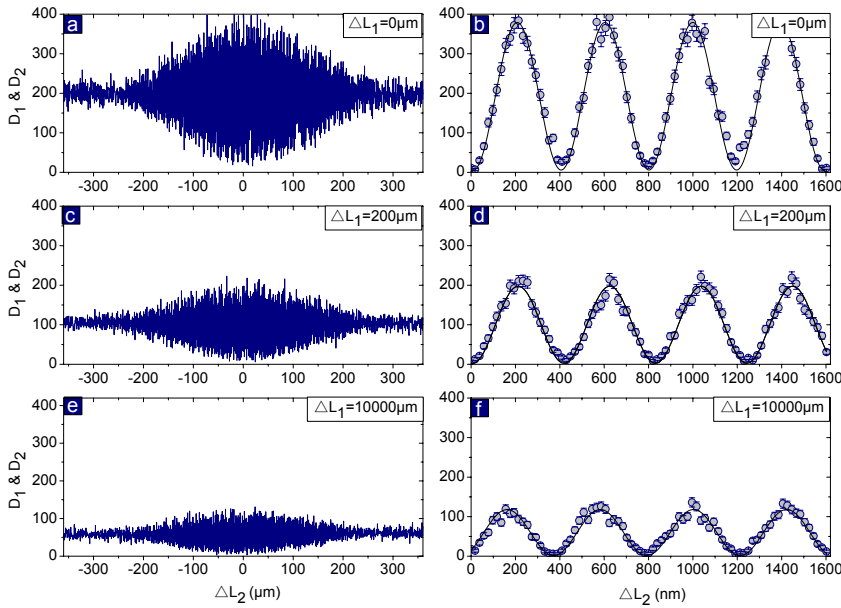


**Figure 3.** Two-photon interference envelope and fringes versus interval  $\Delta L_2$ . Error bars are given by Poissonian statistics. (a)(b).  $\Delta L_1 = 0 \mu m$ . (c)(d).  $\Delta L_1 = 200 \mu m$ . (e)(f).  $\Delta L_1 = 1000 \mu m$ .

#### 4. Discussion

This experiment was finished in May 2008 when one of us (XJ) was working on Ref.[19]. Thanks to Refs.[14], we become aware that our experimental results are of significant scientific values. Meanwhile, we also realized that our experiment could have been further improved. 1), the function of BS1 is just like an optical mixer. In principle, it can be replaced by an optical switch or a WDM (wavelength-division multiplexing). Accordingly, the efficiency of generating the state by Eq. (2) can be optimal  $p = 1$ . 2), one could have tried to increase the interval  $\Delta L_1$  further to mimic the limiting case  $\Delta L_1 \gg 0$ , discussed at the beginning of Section 3.3.

It is already known that the coherent length of a NOON state is normally much larger than the associated single-photon coherent length. This is demonstrated by the interference envelope in Fig. 1e, which is for  $\Delta L_1 = 0$  where the two photons are not distinguishable. Nevertheless, for  $\Delta L_1 \gg \xi$ , the wave packets of the two photons are far apart from each other, and thus they can be distinguished by their spatial positions. For instance, the interference at BS2 seems to depend on the overlap of the single-photon wave packets from paths P5 and P6. In this case, it is not clear (at least to us) whether the coherent length is still much larger than the single-photon coherent length. Therefore, we also measured the whole interference envelopes for  $\Delta L_1 = 0, 200 \mu m$ , and  $1000 \mu m$ . There are shown in Fig. 3, which suggests that, like the interference periodicity, the coherent length of the entangled pair does not depend on the interval  $\Delta L_1$ .

Finally, we mention that the present experimental setup can be equally well used for the  $N$ -photon GHZ state[18]  $1/\sqrt{2}(|H\rangle_1|H\rangle_2 \cdots |H\rangle_3 + |V\rangle_1|V\rangle_2 \cdots |V\rangle_N$ . The periodicity of the associated interference will become  $\lambda/N$ , and thus can be used for quantum-enhanced measurement. In comparison with the conventional MZ interferometer, it alleviates the requirement that the involved photons should arrive simultaneously at the first BS. Actually, it also provides a way to generate a NOON state from a GHZ state.

## Acknowledgements

We are grateful for insightful discussions with Y. Yamamoto. This work was also supported by the National Natural Science Foundation of China and China Postdoctoral Science Foundation.

## References

- [1] Giovannetti, V. Lloyd, S. Maccone, L. *Science* **306**, 1330 (2004).
- [2] Boto, A. et al. Quantum interferometric optical lithography: Exploiting entanglement to beat the diffraction limit. *Phys. Rev. Lett.* **85**, 2733-2736 (2000).
- [3] Kok P. et al. Quantum-interferometric optical lithography: Towards arbitrary two-dimensional patterns. *Phys. Rev. A* **63**, 063407 (2001).
- [4] Holland, M. J. & Burnett, K. Interferometric detection of optical phase shifts at the Heisenberg limit. *Phys. Rev. Lett.* **71**, 1355-1358 (1993).
- [5] Bollinger, J. J., Itano, W. M., Wineland, D. J. & Heinzen, D. J. Optimal frequency measurements with maximally correlated states. *Phys. Rev. A* **54**, R4649-R4652 (1996).
- [6] Ou, Z. Y. Fundamental quantum limit in precision phase measurement. *Phys. Rev. A* **55**, 2598-2609 (1997).
- [7] Jacobson, J., Björk, G., Chuang, I. & Yamamoto, Y. Photonic de Broglie waves. *Phys. Rev. Lett.* **74**, 4835-4838 (2002).
- [8] Braginsky, V. B. Vorontsov, Y. I. *Sov. Phys. Usp.* **17**, 644 (1975).
- [9] Fonseca, E. J. S., Monken, C. H. & Padua, S. Measurement of the de Broglie wavelength of a multiphoton wave packet. *Phys. Rev. Lett.* **82**, 2868-2871 (1999).
- [10] Ou, Z. Y., Wang, L. J., Zou, X. Y. & Mandel, L. Evidence for phase memory in two-photon down conversion through entanglement with the vacuum. *Phys. Rev. A* **41**, 566-568 (1990).
- [11] Rarity, J. G. Two-photon interference in a Mach-Zehnder interferometer. *Phys. Rev. Lett.* **65**, 1348-1351 (1990).
- [12] Edamatsu, K., Shimizu, R. & Itoh, T. Measurement of the photonic de Broglie wavelength of entangled photon pairs generated by spontaneous parametric down-conversion. *Phys. Rev. Lett.* **89**, 213601 (2002).
- [13] Nagata, T. et al. Beating the standard quantum limit with four-entangled photons. *Science* **316**, 726-729 (2007).
- [14] Walther, P. et al. De Broglie wavelength of a non-local four-photon state. *Nature* **429**, 158 (2004).
- [15] Mitchell, M. W., Lunde J. S. & Steinberg, A. M. Super-resolving phase measurements with a multiphoton entangled state. *Nature* **429**, 161 (2004).
- [16] Hong, C. K., Ou, Z. Y. & Mandel, L. Measurement of subpicosecond time intervals between two photons by interference. *Phys. Rev. Lett.* **59**, 2044 (1987).
- [17] Kwiat, P. G. et al. New high intensity source of polarization-entangled photon pairs. *Phys. Rev. Lett.* **75**, 4337-4341 (1995).
- [18] Boumeester, D. et al. Observation of Three-Photon Greenberger-Horne-Zeilinger Entanglement. *Phys. Rev. Lett.* **82**, 1345C1349 (1999)
- [19] Jin, X. M. et al. Experimental Free-Space Quantum Teleportation. *Nature Photonics* DOI: 10.1038/nphoton.2010.87 (2010).